

Local cluster aggregation models of explosive percolation

Raissa M. D'Souza^{1,2} and Michael Mitzenmacher³

¹University of California, Davis, CA 95616, USA

²Santa Fe Institute, 1399 Hyde Park Road, Santa Fe, New Mexico 87501, USA*

³School of Engineering and Applied Sciences, Harvard University, Cambridge, Massachusetts, USA†

We introduce perhaps the simplest models of graph evolution with choice that demonstrate discontinuous percolation transitions and can be analyzed via mathematical evolution equations. These models are *local*, in the sense that at each step of the process one edge is selected from a small set of potential edges sharing common vertices and added to the graph. We show that the evolution can be accurately described by a system of differential equations and that such models exhibit the discontinuous emergence of the giant component. Yet, they also obey scaling behaviors characteristic of continuous transitions, with scaling exponents that differ from the classic Erdős-Rényi model.

PACS numbers: 64.60.ah, 64.60.aq, 89.75.Hc, 02.50.Ey

The percolation phase transition on both lattices and networks is a subject of intense study, as it provides a model for the onset of large-scale connectivity in random media, such as resistor networks, porous rocks, forest fires, and even social networks [1, 2]. It was recently shown via numerical simulation of graph evolution obeying an Achlioptas process that percolation transitions can be discontinuous [3]. Starting from a graph of isolated nodes, at each step of the evolution, two potential edges are chosen uniformly at random, and using some pre-set criteria one edge is added to the graph and the other discarded. If the edge which minimizes the product or sum of the size of the two components that would be merged is chosen, then one can show the percolation transition is discontinuous. Specifically, the size of the largest component goes from sub-linear in system size n to a large fraction (bounded away from 0) of the entire network as a sub-linear number (n^l , with $l < 1$) of edges are added to the graph. Although several recent papers have explored the intuition for the mechanisms behind this behavior, such as identifying that the evolution in the subcritical regime must keep larger components of similar size [4–8], there are not yet mathematical evolution equations describing the process.

In contrast, more restricted Achlioptas processes evolving under “bounded size rules” can be described mathematically. Such rules are constrained so that all components of size greater than some cutoff are treated equivalently. In [9] it was rigorously shown that graph evolution under bounded size rules can be accurately described in terms of differential equations. It is not known, however, whether the restriction to bounded size rules leads to continuous or discontinuous percolation transitions.

Here we introduce and analyze graph evolution models with choice that are both more physically motivated and simpler mathematically. In contrast to those in [3], our models are *local* in the sense that the choice is constrained

to involve edges that share one vertex in common. Thus, the candidate edges span up to three components (rather than four as in [3]). We develop a system of differential equations describing the evolution of the components under the associated bounded size rules, which for the simplest model show that the system must reach a critical point. We implement our equations numerically and find they accurately predict the location of the percolation transition for the case of unbounded rules, and demonstrate via simulation that the transition for unbounded rules is discontinuous.

We explicitly analyze two distinct local processes, although our approach can naturally be used to examine other similar processes. We call the simplest the adjacent edge (AE) rule: at each step, a first vertex is chosen uniformly at random, and it must connect to one of two distinct additional vertices also chosen uniformly at random (thus both candidate edges are adjacent). Intuitively, the first vertex is forced to connect to one of two random choices. Here we choose the edge that connects it to the additional vertex in the smaller component, except possibly in the asymptotically negligible case where the first vertex is in the same component as one of the other two (discussed in detail below). Typical evolution of the largest component of the graph, denoted C_1 , is shown in Fig. 1. In the bounded size rule version, the same rule above is applied unless both components for the two additional vertices have size larger than some bound K . In that case, we simply connect to the first of the two additional vertices.

We follow the approach of Spencer and Wormald [9]. We start with an empty graph G of n vertices. Let $x_i(G)$ be the fraction of vertices in components of size i :

$$x_i(G) = \frac{1}{n} |\{v : c(v) = i\}|, \quad (1)$$

where $c(v)$ is the size of the component containing v . Note that $x_i(G) = in_i(G)$, where $n_i(G)$ is the component density (number of components of size i divided by the system size n) often used in cluster aggregation models in the physics literature [6, 10]. For bounded size variations we will be interested in $x_i(G)$ for $i \leq K$.

*Electronic address: raissa@cse.ucdavis.edu

†Electronic address: michaelm@eecs.harvard.edu

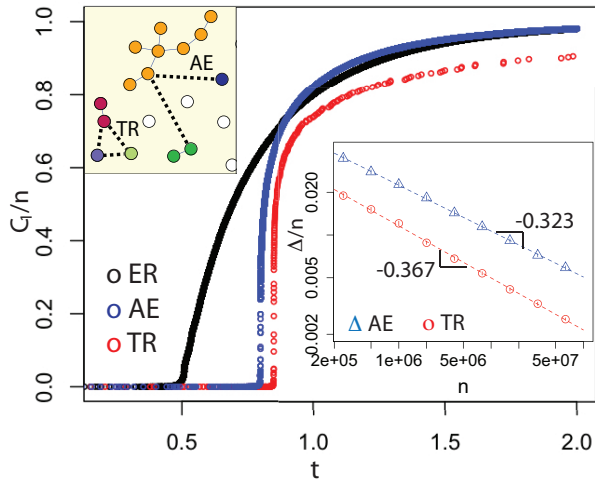


FIG. 1: Typical evolution of C_1/n for Erdős-Rényi (ER), Adjacent Edge (AE), and Triangle Rule (TR), for $n = 10^6$. (Top inset: Example of three candidate edges for TR, and two candidate edges for AE.) (Bottom Inset: $\Delta_n(1/2, 0.2)/n$ vs n for AE and $\Delta_n(1/2, 0.4)/n$ vs n for TR. Each data point is the average over 50 iid realizations, with error bars smaller than symbols. Dashed lines are $\Delta/n = 1.95n^{-0.323}$ for AE and $\Delta/n = 1.84n^{-0.367}$ for TR.)

We provide a mean-field analysis over all graph evolutions. Hence x_i becomes a function of time, $x_i(t)$, where we scale so that a unit of time 1 corresponds to n edges; we suppress the dependence on t where the meaning is clear. We also use $s_j = 1 - \sum_{k < j} x_k$; that is, s_j is the weight of the tail of the distribution starting from j . The probability the first vertex is in a component of size i is x_i . The probability that the smaller of the two additional components has size j is $s_j^2 - s_{j+1}^2 = 2x_j s_j - x_j^2$. Hence, for $1 \leq i \leq K$, we have the differential equations:

$$\frac{dx_i}{dt} = -ix_i - i(s_i^2 - s_{i+1}^2) + i \sum_{j+k=i} x_j(s_k^2 - s_{k+1}^2). \quad (2)$$

This family of equations captures the distribution up to the bound K ; the total fraction of vertices in components of size larger than K is captured by $s_{K+1} = 1 - \sum_{i=1}^K x_i$.

To find the point where the phase transition occurs we consider the evolution of the second moment of the component sizes, which we denote by W . (Again, the dependence on t is implicit.) We define $W = \frac{1}{n} \sum_v c(v)$; this is the expected size of the component to which an arbitrary vertex belongs. We may also write $W = \sum_{i=1}^{\infty} i^2 n_i = \sum_{i=1}^{\infty} i x_i = \sum_{i=1}^{\infty} s_i$. It helps notationally to let $W^* = W - \sum_{i=1}^K i x_i$; here W^* corresponds to the contributions to W from vertices in components larger than the bound K . Finally, when components of size j and k are merged, the change in W is equal to

$(j+k)^2 - j^2 - k^2 = 2jk$. The evolution of W is:

$$\begin{aligned} \frac{dW}{dt} = & \sum_{j=1}^K \sum_{k=1}^K 2jkx_j(s_k^2 - s_{k+1}^2) + \sum_{j=1}^K 2jW^*x_j s_{K+1} \\ & + \sum_{k=1}^K 2kW^*(s_k^2 - s_{k+1}^2) + 2(W^*)^2 s_{K+1}. \end{aligned} \quad (3)$$

The four terms can be explained as follows. 1) Both components have size $\leq K$: the change in W is $2jk$ multiplied by the respective probabilities that the first vertex has component size j and the smaller of other two components has size k . 2) The first vertex has component size $j \leq K$; the second is larger than K . (Note that the sum $\sum_{k=K+1}^{\infty} kx_k$ simplifies to W^* , which we have used to simplify the expression.) 3) The first vertex has component size greater than K and the second does not. 4) All three components have size greater than K .

As $\sum_{j=1}^K jx_j = W - W^*$, we can simplify to obtain

$$\frac{dW}{dt} = 2W \sum_{k=1}^K k(s_k^2 - s_{k+1}^2) + 2WW^* s_{K+1}, \quad (4)$$

which can be used to show that this bounded size rule must eventually reach a critical point where W grows to infinity. Specifically, since $s_k \geq s_{k+1}$,

$$\frac{dW}{dt} \geq 2WW^* s_{K+1}. \quad (5)$$

Consider the first point where $s_{K+1} \geq \epsilon$ for some constant $\epsilon > 0$. (Since we keep adding edges, and K is a constant, it is straightforward to show that s_{K+1} must eventually grow larger than a suitably small constant ϵ .) At this point $W^* \geq \epsilon W$ (since the at least ϵ fraction of W from large components must contribute at least ϵW of W^* 's value), implying $\frac{dW}{dt} \geq 2\epsilon^2 W^2$, from which it follows that W goes to infinity at some finite time.

It is tempting (but somewhat unrigorous) to consider the limiting version of these eqns without the bound K :

$$\frac{dW}{dt} = 2W \sum_{k=1}^{\infty} s_k^2 > 2W. \quad (6)$$

It is not immediately clear how to use Eq. 6 to similarly demonstrate a critical point for the unbounded case.

Further details need to be dealt with to formalize the accuracy of the differential equations; here we refer the reader to [9], which provides a full treatment for the case where two independent edges are chosen for each step. In particular, a key issue is that the differential equations fail to take into account redundant steps, where an edge joins two vertices that are already in the same component. The behavior for the x_k 's is relatively straightforward under bounded-size rules; the probability that two vertices chosen at random fall in the same component of size at most K is $O(K^2/n)$, and the asymptotic effect

of such deviations does not affect convergence to the differential equations. The argument is more challenging for bounding the effect on W , as W 's growth involves components of size larger than K ; however, by showing that the fraction of vertices in components of size k with high probability eventually falls geometrically with k (as detailed in [9]), similar bounds can be shown to hold.

One additional benefit of considering local schemes is that various generalizations are entirely transparent. For example, the extension to d choices of neighbors of the first vertex instead of two for a given integer d yields

$$\frac{dx_i}{dt} = -ix_i - i(s_i^d - s_{i+1}^d) + i \sum_{j+k=i} x_j (s_k^d - s_{k+1}^d); \quad (7)$$

$$\frac{dW}{dt} = 2W \sum_{k=1}^K k(s_k^d - s_{k+1}^d) + 2WW^* s_{K+1}^{d-1}. \quad (8)$$

Again, the limiting variation as K goes to infinity has the simpler form $\frac{dW}{dt} = 2W \sum_{k=1}^{\infty} s_k^d$.

The second process we study (suggested in [4, 11]) is the triangle rule (TR): at each step choose three distinct vertices uniformly at random, examine the triangle of three possible edges connecting the pairs of vertices, and select the edge that connects the two smallest components. Typical evolution of C_1 for this process is shown in Fig. 1. The bounded size rule variant is that if all components have size above the bound K , we choose a random edge from the three; if two components have size above the bound K , we choose a random edge from the two adjacent to the smallest component. Using the same notation and analysis approach as for the AE rule, we can find differential equations for the bounded size variant;

$$\begin{aligned} \frac{dx_i}{dt} = & -2ix_i^3 - 6ix_i^2 s_{i+1} - 3ix_i^2(1 - s_i) - 3ix_i s_{i+1}^2 \\ & - 6ix_i s_{i+1}(1 - s_i) + 6i \sum_{j+k=i; j < k} x_j x_k s_{k+1} \\ & + ix_{i/2}^3 + 3i \sum_{j+k=i; j < k} x_j x_k^2 + 3ix_{i/2}^2 s_{i/2+1}. \end{aligned} \quad (9)$$

We briefly explain each term of Eq. 9. 1) All components have size i ; $2i$ vertices lost. 2) Two components have size i , one has size greater than i . 3) Two components have size i , one has size less than i . 4) One component has size i , and two have size larger than i . 5) One component has size i , one has size less than i , one has size greater than i . 6) All three components have different sizes, and the smallest two sum to i . 7) All three components have size $i/2$. (This term only appears when i is even.) 8) The two largest components have equal size, and the smallest two sum to i . 9) The two smallest components have equal size and sum to i . (This term only appears when i is even.) Explaining, for example, the second term in more detail: we lose $2i$ vertices from x_i when two components have size i and one has size greater than i , and the probability of this is $3x_i^2 s_{i+1}$ when we take into account the orderings of the choices.

We again analyze how $W = \frac{1}{n} \sum_v c(v)$ changes:

$$\begin{aligned} \frac{dW}{dt} = & \sum_{j=1}^{K-1} \sum_{k=j+1}^K 12jkx_j x_k s_{k+1} + \sum_{j=1}^K \sum_{k=j+1}^K 6jkx_j x_k^2 \\ & + \sum_{j=1}^{K-1} 6j^2 x_j^2 s_{j+1} + \sum_{j=1}^K 2j^2 x_j^3 \\ & + W^* \sum_{j=1}^K 6jx_j s_{K+1} + 2(W^*)^2 s_{K+1}. \end{aligned} \quad (10)$$

The triangle setting lacks the pleasant form of the AE rule, but is suitable for calculation and fairly succinct. Here too, we can similarly create equations for merging the two largest components instead of the two smallest.

For both the adjacent edge (AE) and triangle rule (TR) models, we solve the differential equations numerically using Euler's method in order to calculate, roughly, the location of the phase transition. We discretized time with steps of size 10^{-6} . More sophisticated approaches using higher precision and error bounds could yield more precise values, but the simple approach is sufficient for our current purposes. For the AE model, using a value of $K = 400$ led to an explosion in W occurring between times 0.794 and 0.795; for $K = 600$, the explosion occurred slightly later, between times 0.795 and 0.796. For the TR model, at $K = 400$ the explosion occurred between times 0.847 and 0.848, and for $K = 600$ it occurred between times 0.848 and 0.849. This closely matches the results from direct simulation of the graph evolution processes discussed next.

We establish the explosive nature of the transition for both the AE and TR models via numerical simulation of the underlying graph processes. We follow the approach introduced in [3], while here providing a more formal and detailed explanation of the procedure. Let $\Delta_n(\gamma, A)$ denote the number of edges required for C_1 to go from size $C_1 \leq \lfloor n^\gamma \rfloor$ to size $C_1 \geq \lfloor An \rfloor$, for a system of n vertices. We wish to understand the asymptotic behavior, $\lim_{n \rightarrow \infty} \Delta_n(\gamma, A)$. If $\Delta_n(\gamma, A)$ increases linearly with n , then the time difference spanned by the window, $\Delta_n(\gamma, A)/n$, approaches a limiting constant greater than zero (the slope of $\Delta_n(\gamma, A)$ versus n). If, in contrast, $\Delta_n(\gamma, A) \propto n^\beta$ with $\beta < 1$ (i.e., $\Delta_n(\gamma, A)$ is sublinear in n), then $\Delta_n(\gamma, A)/n \rightarrow 0$ as $n \rightarrow \infty$. In other words C_1 goes from size n^γ to size An in a time difference which approaches zero (shown for AE and TR in Fig. 2(a)).

As shown in the inset to Fig 1, for the AE model we find that $\Delta_n(0.5, A) \sim n^{0.68}$ for all $A \in [0.1, 0.3]$. For the TR model we find $\Delta_n(0.5, A) \sim n^{0.63}$ for all $A \in [0.1, 0.4]$. The lower bound should decrease as we access larger n . The upper bound estimates the largest value of A for which the scaling is sublinear, denoted A_c . Formally, $A_c = \sup_A [\lim_{n \rightarrow \infty} \Delta_n(\gamma, A)/n \rightarrow 0]$, which is the size of the discontinuous jump in C_1/n when viewed within this scaling window.

We can bound the critical point for each process using the upper and lower boundaries of $\Delta_n(\gamma, A)$. Namely,

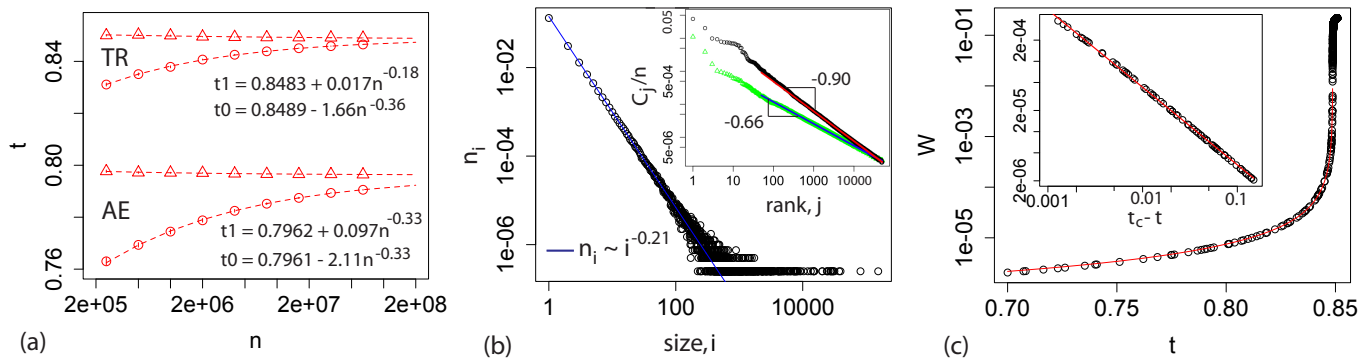


FIG. 2: (a) Measuring the lower and upper boundaries of $\Delta_n(1/2, 0.2)/n$ for AE and $\Delta_n(1/2, 0.4)/n$ for TR. (b) Component density $n_i \sim i^{-2.1}$ shown for AE at t_c (TR and PR are similar). More interesting is the rank-size component distribution (inset for ER and AE at t_c), showing the preponderance of large components for AE. Fitting for $50 < j < 50,000$ yields $C_j \sim j^{-\delta}$, with $\delta = -0.66$ for ER and $\delta = -0.90$ for AE (TR and PR are similar but more noisy). (c) W versus t for TR. Inset shows $W \sim (t_c - t)^{-\alpha}$ with red-line showing the best fit, attained with $\alpha = 1.13$. The same red line is depicted in the main figure.

we measure how t_0 , the last time for which $C_1 \leq n^\gamma$, and likewise how t_1 , the first time for which $C_1 \geq An$, depend on n . As shown in Fig. 2(a), we find that t_0 and t_1 approach essentially the same limiting value denoted t_c . Neither of these local models is as effective in delaying the onset of the giant component as the original Product Rule (PR) studied in [3] where the critical point $t_c \approx 0.888$. For AE, $t_c \approx 0.796$, while for TR, $t_c \approx 0.848$. Likewise neither model is as “explosive” since $A_c \approx 0.6$ for PR, $A_c \approx 0.3$ for AE, and $A_c \approx 0.4$ for TR. Other well-known processes have now been shown to have discontinuous Achlioptas process counterparts [12–14].

The discontinuous jump in the order parameter C_1 is characteristic of first order phase transitions. Yet, we observe critical scaling characteristic of second order transitions. Figure 2(b) shows that n_i , the scaled number of components of size i , behaves as $n_i \sim i^{-\tau}$, with $\tau = 2.1$ for both AE and TR (matching recently reported results for PR [6, 8, 15]). Figure 2(c) shows how W diverges at the critical point, behaving as $W \sim |t - t_c|^{-\alpha}$. We also see similar behavior for the size of the second largest component, $C_2 \sim |t - t_c|^{-\mu}$. Our numerical estimates are

$\alpha = \mu \approx 1.13$ for AE and TR, while $\alpha = \mu \approx 1.17$ for PR. Note, we recover the standard Erdős-Rényi (ER) exponents ($\tau = 5/2$ and $\alpha = \mu = 1$) in our simulations of ER. Hybrid phase transitions have been previously observed for spin glasses [16, 17], constraint satisfaction problems (K-SAT) [18], models of jamming in granular materials (see [19–21] and references therein), and k -core percolation [22].

In summary we have introduced local models of graph evolution with choice that can be described by mathematical evolution equations and which exhibit discontinuous percolation transitions with critical scaling behaviors. Discontinuous percolation transitions are not yet fully understood. Local processes appear much simpler to describe mathematically and thus offer the potential for a system with a discontinuous percolation transition that is easier to analyze.

We thank Microsoft Research New England where this research was initiated. R.D. was supported in part by National Academies Keck Futures Initiative grant CS05 and M.M. by NSF grants CCF-0634923 and CCF-0915922.

-
- [1] D. Stauffer and A. Aharony. *Introduction to Percolation Theory* (Taylor & Francis, London, 1994).
[2] S. Solomon, G. Weisbuch, L. de Arcangelis, N. Jan and D. Stauffer. *Physica A*, 277(1-2):239–247, 2000.
[3] D. Achlioptas, R. M. D’Souza, and J. Spencer. *Science*, 323(5920):1453–1455, 2009.
[4] E. J. Friedman and A. S. Landsberg. *Phys. Rev. Lett.*, 103:255701, 2009.
[5] A. A. Moreira, E. A. Oliveira, S. D. S. Reis, H. J. Herrmann, and J. S. Andrade Jr. *arXiv:0910.5918*.
[6] Y. S. Cho, B. Kahng, and D. Kim. *Phys. Rev. E* 81, 030103(R) (2010).
[7] H. D. Rozenfeld, L. K. Gallos, and H. A. Makse. *arXiv:0911.4082*.
[8] S. S. Manna and A. Chatterjee. *arXiv:0911.4674*.
[9] J. Spencer and N. Wormald. *Combinatorica*, 27(5):587–628, 2007.
[10] E. Ben-Naim and P. L. Krapivsky. *Phys. Rev. E*, 71:026129, 2005.
[11] P. L. Krapivsky. Private communication. Oct. 24, 2007.
[12] R. M. Ziff. *Phys. Rev. Lett.*, 103:045701, 2009.
[13] F. Radicchi and S. Fortunato. *Phys. Rev. Lett.*, 103:168701, 2009.
[14] Y. S. Cho, J. S. Kim, J. Park, B. Kahng, and D. Kim. *Phys. Rev. Lett.*, 103:135702, 2009.
[15] F. Radicchi and S. Fortunato. *Phys. Rev. E* 81, 036110 (2010).
[16] D. Gross and M. Mezard. *Nucl. Phys. B*, 240:431–452,

- 1984.
- [17] T. R. Kirkpatrick and D. Thirumalai. *Phys. Rev. Lett.*, 58:2091, 1987.
- [18] R. Monasson, R. Zecchina, S. Kirkpatrick, B. Selman, and L. Troyansky. *Nature*, 400:133137, 1999.
- [19] C. S. O'Hern, S. A. Langer, A. J. Liu, and S. R. Nagel. *Phys. Rev. Lett.*, 88:075507, 2002.
- [20] C. Toninelli, G. Biroli, and D. S. Fisher. *Phys. Rev. Lett.*, 96:035702, 2006.
- [21] J. M. Schwarz, A. J. Liu, and L. Q. Chayes. *Europhys. Lett.*, 73(4):560, 2006.
- [22] S. N. Dorogovtsev, A. V. Goltsev, and J. F. F. Mendes. *Phys. Rev. Lett.* 96, 040601 (2006).